Influence of Coulomb effects on the resolving power of multireflection mass-spectrometer systems

M.G. Skoblin, I.A. Kopaev, D.E. Greenfield, A.A. Makarov, M.A. Monastyrskiy, S.S. Alimpiev

Abstract. General theoretical approaches to the modelling of Coulomb effects in short ion bunches, developed previously by the authors, are applied in this paper to the calculation of multireflection mass-spectrometer systems. A separate module of the MASIM 3D applied software package is designed. An adaptive computational procedure for calculating the 'mirror potential' induced by an ion bunch on the surface of field-forming electrodes is proposed. The dynamics of ion bunches in a time-of-flight reflectron-type mass analyser is calculated and the limitations on the resolving power, caused by resonant Coulomb effects of self-bunching and coalescence in the groups of particles with close masses, are revealed on the basis of numerical experiments.

Keywords: multireflection mass-spectrometer system, Coulomb interaction, perturbation theory, self-bunching and coalescence of ion bunches.

1. Introduction

One can outline two major factors that determine the resolving power of mass spectrometers. The first factor is related to the ion bunch flight length in a mass spectrometer, whilst the second one is stipulated by the Coulomb interaction of charged particles within the bunch.

The first factor is well-studied and represents a subject of a considerable number of works and inventions. The problem of increasing the flight length has been effectively solved by means of ion mirrors in which ions multiply oscillate, herewith residing within a restricted volume. Mamyrin et al. [1] proposed the use of a reflectron-type mass analyser capable of compensating for the spread of ions in initial energies, which ensured a significant advance in the resolving power.

M.G. Skoblin Tal'roze Institute of Energy Problems for Chemical Physics (Chernogolovka Branch), Russian Academy of Sciences, prosp. Akad. Semenova 1/10, 142432 Chernogolovka, Moscow region, Russia; e-mail: skoblin.michael@gmail.com;
I.A. Kopaev, M.A. Monastyrskiy A.M. Prokhorov General Physics Institute, Russian Academy of Sciences, ul. Vavilova 38, 119991 Moscow, Russia;
e-mail: igorkopaev@gmail.com, misha-monast@yandex.ru;
D.E. Greenfield, A.A. Makarov ThermoFisher Scientific (Bremen) GmbH, Hanna-Kunath-Str. 11, 28199 Bremen, Germany;
e-mail: dmitry.grinfeld@thermofisher.com;
S.S. Alimpiev A.M. Prokhorov General Physics Institute, Russian Academy of Sciences, ul. Vavilova 119991, Moscow, Russia; LLC 'New Energy Technologies', ul. Novaya 100, 143025 Skolkovo, Moscow region, Russia, e-mail: sergey.alimpiev@mail.ru

Subsequently, various variants of multireflection systems have been developed, with an ion bunch oscillating between two or more electrostatic mirrors. In particular, a multireflection mass analyser with two axially symmetric ion mirrors separated by a field-free space was designed by the authors of [2]. Optimisation of the geometry of mirrors and supply voltages provides for the ion motion isochronism, i.e. independence of the period of oscillations on the initial parameters. As was shown later [3], a special choice of geometric parameters of ion mirrors allows eliminating the time-of-flight (TOF) chromatic aberrations up to the third order inclusive and at the same time ensures a spatial stability of the ion bunch for an arbitrary large number of oscillations between the mirrors. The authors of [4, 5] proposed a new design of a TOF mass analyser with two extended ion mirrors being parallel to each other. In this instrument, the ion bunch makes multiple isochronous oscillations between the mirrors and simultaneously drifts along the mirrors. A system of electrostatic einzel lenses prevents the bunch disintegration in the drift direction. A mass-spectrometer system comprising a mirror and a set of extended orthogonal mirrors was developed in [6]. This design does not require additional lenses, and the off-axis TOF aberrations are automatically eliminated in this system due to the fourfold symmetry of the phase space. An orbital electrostatic trap with a so-called 'quadro-logarithmic' field possessing ideal isochronous properties was proposed in [7]. The same field distribution was used in the energy analyser [8] and also in the Orbitrap Fourier transform mass spectrometer [9]. Afterwards, the unique properties of the 'quadro-logarithmic' field have been used in the multireflection TOF mass analyser [10].

The works cited above do not take into account the Coulomb effects in their simulation of real mass-spectrometer systems. However, even if the ion mirror design is ideal in terms of TOF aberrations, the allowable number of ions in the bunch turns out significantly limited by space-charge effects.

The second factor mentioned above, indicating the need of addressing the Coulomb interaction effects between charged particles, becomes of particular importance for modern mass-spectrometer systems based on highly efficient ionisation methods employing laser radiation [11–19]. These methods include the MALDI method (Matrix Assisted Laser Desorption/Ionisation), which is based on desorption and ionisation of chemicals compounds by means of pulsed laser radiation with the use of an organic matrix and possesses an effective ionisation probability of $10^{-5}-10^{-6}$ [13, 14]; the SALDI method (Surface Assisted Laser Desorption/Ionisation), which employs the laser desorption of ions from the specially

prepared rough surfaces with an ionisation probability of $10^{-2} – 10^{-3}$ [18]; and the APLPI method (Atmospheric Pressure Laser Plasma Ionisation), based on the ionisation of organic compounds by means of emission from laser plasma at atmospheric pressure, also possessing a high ionisation probability [19].

The use of highly efficient laser ionisation methods makes very urgent the solution of the problem of allowance for the Coulomb effects in dense ion bunches generated by such sources, because only in this case we may rely on obtaining a reliable knowledge on the limiting resolving power of modern mass-spectrometer systems. For example, a remarkable effect, which, at a first glance, seems quite paradoxical, is peculiar to reflectron-type systems. Subjected to the Coulomb interaction, ions of identical type with identical mass-to-charge ratio possess an equal period of oscillations despite the initial energy spread and the presence of the field perturbations violating the isochronism condition. The nature of this synchronisation effect of ion oscillation (self-bunching) is due to the resonant nature of the Coulomb interaction, which is inherent in the oscillatory motion of an ensemble of charged particles. It is worth noting that a manifestation of this synchronisation effect in a system of two weakly coupled oscillators was known to Christiaan Huygens [20], who called it an "odd sympathy".

Despite the fact that the self-bunching effect reduces the spread of particles with the same mass-to-charge ratio, it does not contribute to the enhancement of the resolving power because the self-bunching effect is always accompanied by the effect of charged particle coalescence. From the viewpoint of charged particle dynamics, the coalescence effect represents a manifestation of the self-bunching effect for the groups of ions with close m/z ratios. Indeed, let us consider two 'mass peaks', each of them comprising a large number of identical ions with a mass-to-charge ratio of ions in both peaks being very close. If the self-bunching effect prevails over the effect of the mass-peaks separation due to the transit time and multiple reflections, both types of particles will move between the mirrors as a single bunch. In this case, the mass-peaks of ions could not be resolved even after an arbitrarily large number of oscillations. Obviously, from a practical viewpoint, the coalescence effect defines a 'Coulombian' limit of the resolving power in a mass spectrometer, and it is extremely important to determine a set of conditions responsible for manifestation of this effect.

Mathematical modelling of the above phenomena is very sophisticated and requires an accurate enough evaluation of the Coulomb interaction contribution to the ion bunch motion against the background of external electric fields. A vast majority of the known works [21–27] have been studying these effects either experimentally or using relatively simple models capable of clarifying the essence of the phenomena on a qualitative level only. These models can hardly be considered as a reliable basis for the creation of a modern computational framework for the design and optimisation of mass spectrometers with a real complicated geometry.

The computational algorithms for solving the problems of Coulomb dynamics as applied to high-resolution mass spectrometry, outlined in this paper, represent an integral part of our MASIM 3D software package [28]. The approach combines a special procedure for calculating ion trajectories with the use of perturbation theory and Barnes–Hut method [29] that is borrowed from the celestial mechanics. The essence of the approach is to decompose the original system of

motion equations into two interconnected systems of equations [30, 31]. One of these systems comprises only external (smooth) fields, and, consequently, its solution may be represented in the form of an aberrational expansion, whilst the other one contains explicitly only the Coulomb (non-smooth) potential, the electric field of which is commonly several orders of magnitude smaller than the external field produced by the system of the electrodes. Thus, 'large' and 'small' field items appearing in the original system of the motion equations turn out separated, which ensures high accuracy and stability of the whole process of calculating the trajectories with regard to the Coulomb interaction.

Calculations and experiments show that the ion bunch may pass near the system boundaries. In that case, to adequately describe the dynamics of the ion ensemble, the 'mirror-image' field, which appears due to the interaction of the ion bunch with the nearby electrodes, should be necessarily taken into account. Below we formulate a special algorithm that allows an adaptive solution of a relevant boundary-value problem in the course of the bunch motion.

The first part of this work is dedicated to the construction of computational algorithms and software for solving numerically the problems of high-resolution mass spectrometry in the case of 3D geometry of the field-forming electrodes with allowance for Coulomb effects. All the algorithms outlined below are implemented as a separate software module being a part of the MASIM 3D applied program package.

In the second part, this software is used for simulation of the resonant Coulomb effects of self-bunching and coalescence in a TOF reflectron-type mass spectrometer, to assess the impact of these effects on the limiting resolving power of such instruments.

2. The Coulomb potential calculation using the modified Barnes–Hut method

Direct calculation of the Coulomb potential created by N particles having charges q_p and radius vectors $\boldsymbol{R}_p$ ($p = 1, .., N$) at a fixed point with a radius vector $\boldsymbol{S}$ assumes the summation of N terms,

$$\varphi(\boldsymbol{S}) = \sum_{p=1}^{N} \frac{q_p}{|\boldsymbol{S} - \boldsymbol{R}_p|}, \qquad (1)$$

the calculation of which requires the execution of a great number of time-consuming operations. If we want to know the Coulomb field of each particle of interest at every step of integration of the motion equations, we have to calculate as many as $N(N-1)/2$ of such terms for all possible pairs of particles that form a bunch. For sufficiently large N, such a calculation becomes extremely cumbersome even for modern computers.

The calculation speed can be increased if we combine the particles into groups depending on their position relative to the point $\boldsymbol{S}$, considering each of these groups as a single field source.

In 1986, Barnes and Hut [29], with the aim of calculating the gravitational fields of stellar clusters in celestial mechanics, proposed a more effective implementation of the general idea of grouping the particles. Instead of grouping the individual particles with respect to a given point of field calculations, the Barnes–Hut algorithm suggests ranking of the cells of a special tree-like structure which is constructed of the particles comprising the cloud at every step of integration of the

motion equations. Since the mathematical description of the gravitational and Coulomb fields has much in common, this algorithm turned out very promising in computational charged-particle optics. The details of the Barnes–Hut algorithm's version used in this paper, with a computational complexity of $N\log N$ order, can be found in [31].

3. Allowance for the 'mirror image' fields in the Coulomb problems with complicated geometry of electrodes

In practice, dense ion bunches often pass in immediate proximity of field-forming electrodes, so that the potential induced by ions on the conductive surfaces of these electrodes can significantly affect the ion bunch dynamics. Within the framework of the nonrelativistic quasi-stationary approximation, the total electric potential $\varphi(\mathbf{r}, \tau)$ created by the external sources (electrodes) and the Coulomb interaction between the charged particles constituting a moving cloud with particle density $\rho(\mathbf{r}, \tau)$ satisfies the Poisson equation

$$\Delta \varphi = -4\pi \rho(\mathbf{r}, \tau) \tag{2}$$

with the given boundary conditions on the electrode surface Γ

$$\varphi|_{\Gamma} = \varphi(\mathbf{r}_P, \tau), \quad P \in \Gamma. \tag{3}$$

Let us represent the solution of the boundary-value problem (2), (3) as a sum of three terms:

$$\varphi(\mathbf{r}, \tau) = \varphi_0(\mathbf{r}, \tau) + \varphi_C(\mathbf{r}, \tau) + \varphi^*(\mathbf{r}, \tau), \tag{4}$$

where $\varphi_0(\mathbf{r}, \tau)$ is the external potential defined as a solution of the Dirichlet problem for the Laplace equation:

$$\Delta \varphi = 0, \quad \varphi|_{\Gamma} = \varphi(\mathbf{r}_P, \tau), \quad P \in \Gamma; \tag{5}$$

$$\varphi_C(\mathbf{r}, \tau) = \int \frac{\rho(\mathbf{r}', \tau)}{|\mathbf{r} - \mathbf{r}'|} d\mathbf{r}' \tag{6}$$

is the space-charge potential induced by the interaction between the charged particles; and $\varphi^*(\mathbf{r}, \tau)$ is the so-called mirror potential arising from the interaction of charged particles with conductive electrodes and defined as a solution of the Dirichlet problem:

$$\Delta \varphi = 0, \quad \varphi|_{\Gamma} = -\varphi_C(\mathbf{r}_P, \tau). \tag{7}$$

Obviously, the function $\varphi_C^*(\mathbf{r}, \tau) = \varphi_C(\mathbf{r}, \tau) + \varphi^*(\mathbf{r}, \tau)$ satisfies the Poisson equation with zero initial conditions.

As noted above, if a dense bunch of charged particles is moving near the field-forming electrodes, the contribution of the 'mirror-image' potential $\varphi^*(\mathbf{r}, \tau)$ can be very significant.

To solve problem (7), the Barnes–Hut method can be supplemented by a relatively simple and efficient approach for calculating the mirror potential in the form of the harmonic sum

$$\varphi_C^* = \varphi_C + A_{00}$$

$$+ \sum_{n=1}^{N_g} r^n \sum_{m=0}^{n} (A_{nm}\cos\phi + B_{nm}\sin\phi)\, Y_{nm}(\vartheta). \tag{8}$$

Here, (r, ϕ, ϑ) are the spherical coordinates of the radius vector drawn from the ion cloud centre to a given point; N_g is the maximum order of spherical harmonics; and $Y_{nm}(\vartheta)$ is the spherical part of the associated Legendre polynomials. The coefficients A_{nm}, B_{nm} can be found by minimising the quadratic residual (i.e. the squared deviation of the approximating dependence from the desired function)

$$\sum_{k=1}^{M} |\varphi_C^*(r_P, \tau)|^2 \to \min \tag{9}$$

on the finite set M of the boundary points $r_P \in \Gamma$. Solution (8) exactly satisfies the Poisson equation and approximately satisfies the boundary conditions (7). It is easy to see that equation (9) produces a set of linear equations for the coefficients A_{nm}, B_{nm}.

To ensure a required accuracy, the set of boundary points should adequately reflect the geometry of the electrode surfaces. Obviously, the maximal contribution to the mirror potential is provided by the charge induced on the boundary elements being nearest to the bunch. In this regard, to remove the unwanted 'noise' arising from taking into account remote (and therefore insignificant) boundary points, the set M, which is moving with the bunch, only includes the points located within a sphere of a radius R, whose centre coincides with the geometric centre of the ion cloud, and the value of R represents a problem-dependent variable to be determined in numerical experiments.

If the system geometry is complicated enough, some elements of the electrode surface can be shielded (screened) by other elements being 'visible' from the ion cloud centre. The points belonging to such shielded elements are not included into representation (9). A special computational procedure eliminates such shielded elements. The computational model includes six 'cameras' with a field of view of 90°, placed at the ion cloud centre. In the course of the ion cloud motion, each of the 'visible' boundary elements is being projected onto the image plane of the cameras, thus ensuring the adaptive accumulation of the necessary boundary elements to be included into the numerical process of finding the coefficients A_{nm}, B_{nm}.

4. Numerical solution of the test problems

A pithy problem of the Coulomb dynamics of charged particles, which admits a quasi-analytical (exact) solution, is the problem of expansion of a spherical cloud of charged particles in free space, considered earlier in [31, 32]. Figure 1 shows the density evolution of a spherically symmetric bunch of protons, which is calculated using the Barnes–Hut algorithm and according to the exact solution (shaded area). Initially, the protons being in rest are distributed within a sphere of a radius $r_0 = 1$ mm. At the initial time moment $t = 0$, the charged particles that form the cloud start to move due to the Coulomb repulsion.

Below we consider the cases when the initial distribution of the particle density inside the sphere is either uniform (Fig. 1a) or highly nonuniform (Gaussian) (Fig. 1b). It is clearly seen that, in the case of a uniform initial distribution, the particle density remains constant when the sphere expands under the action of Coulomb interaction, whereas, in the case of the nonuniform initial density, the charged particles form density maxima ('overtaking catastrophes') at the forefront of the expanding cloud. This behaviour of the space-charge den-
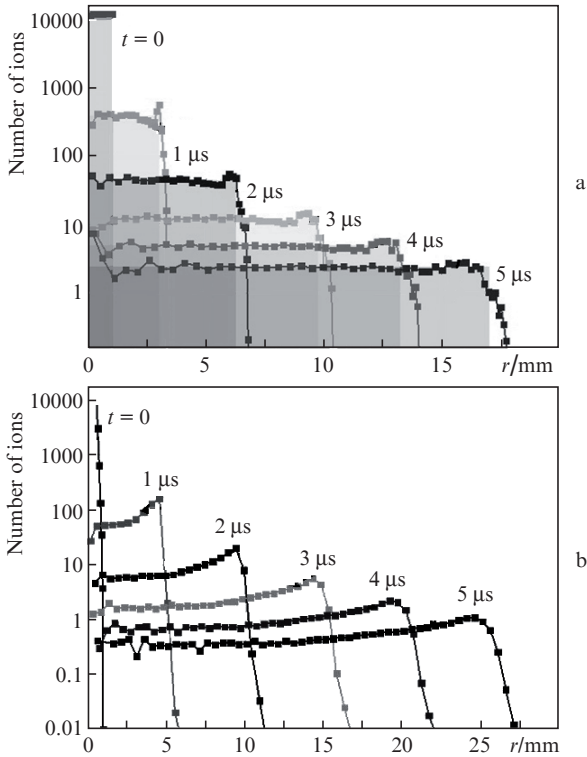
Figure 1. Evolution of a spherically symmetric cloud of protons with (a) initially uniform and (b) initially nonuniform (Gaussian) charge density distribution calculated by means of the Barnes–Hut method (rectangles) and in accordance with the exact solution (grey area in Fig. 1a).

sity is well-consistent with the results obtained in [31, 32] by means of analytical methods.

The main goal of solving the problem considered below is to determine how the modified Barnes–Hut algorithm, complemented by the technique of the mirror-potential calculation, describes the Coulomb dynamics of charged particles in the presence of conductive surfaces. In this test, a uniformly charged sphere with the initial radius $R = 1$ mm is placed inside a cube with a rib length of $L = 20$ mm, so that, at the initial time moment, the sphere centre is distanced by 5 mm from the nearest face of the cube.

At $t = 0$ the sphere begins to expand due to the Coulomb interaction. The difference between the ion cloud motion in a close proximity to the conductive surface and in free space is stipulated by the presence of the mirror charge induced by the ion cloud. As noted above, in the framework of the approach applied, the mirror potential generated by the space charge is taken into account by adding a finite number of terms of the harmonic series (8), whose coefficients are determined by minimising residual (9). It should be emphasised that the problem of calculating the potential induced by the ion cloud surrounded from all sides by conductive electrodes proved to be more stable than the problem with an infinite plane. This reflects the fact that the internal Dirichlet problem is stable (correct) with respect to small variations in the boundary conditions, in contrast to the Cauchy problem for an infinite plane.

If the ion cloud is located sufficiently close to one of the cube faces, we can compare the solution derived by minimising residual (9) (hereinafter referred to as the L_2 approximation) with a solution that takes into account the presence of

two charged clouds – real and imaginary, obtained by the mirror reflection of the real cloud relative to the plane containing the corresponding cube face. As above, the latter solution is called the exact one. Figure 2 shows the potential distribution on the cube face which at $t = 0$ is distanced by 5 mm from the ion cloud centre. The distributions in Figs 2a, 2b and 2c correspond to the solutions with the number of Fourier harmonics in expansion (8) equal to 3, 5 and 7, respectively. The exact solution is shown in Fig. 2d. It can be seen that the L_2 approximation converges to the exact solution when the number of Fourier harmonics grows. Thus, it is shown that the proposed algorithm ensures sufficient accuracy in calculating the mirror potential in the problems with dense ion bunches.
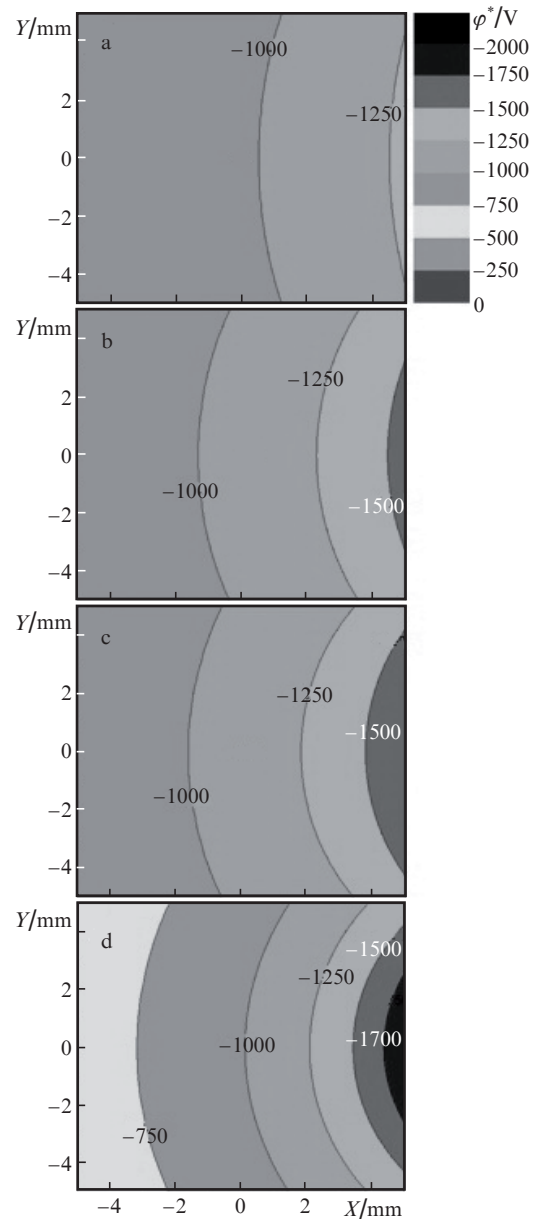

Figure 2. Distribution of the mirror-potential additive in the XY plane, obtained by minimising residual (9) for the test system consisting of a conductive cube and an ion cloud with $N \sim 10^3$, at the number of harmonics (a) 3, (b) 5, (c) 7, and (d) the exact solution having the computational complexity of N^2.

5. Modelling of the Coulomb effects in the TOF reflectron-type mass analyser

The TOF reflectron-type mass analyser we consider below is described in detail in [33]. It consists of two identical axisymmetric mirrors separated by a region with a constant potential. As shown in Fig. 3, each of the mirrors is composed of four ring-shaped electrodes. Three pairs of external (U2 – U4) electrodes have a positive potential for producing a reflective field. The inner pair of electrodes (U1) has a smaller diameter and a negative potential. These electrodes form an accelerating electrostatic lens that provides the transverse stability of the bunch.

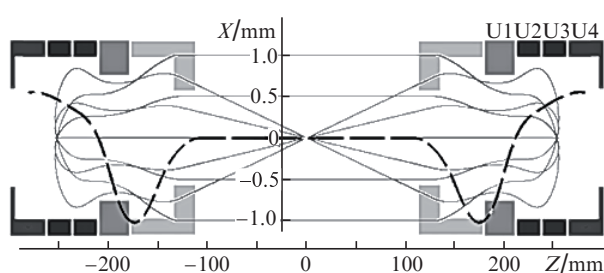The instrument operation process can be provisionally divided into several stages. Originally, the ions derived by means of a standard electrospray-type ion source [11] are injected into a linear high-frequency trap in the form of a low-energy continuous flow. Then, as a result of changing the potentials of external electrodes, the ion bunch is locked in a multireflection trap. After accumulating and cooling of the required amount of ions, the confining potential turns off and the applied electric field pulls the charged particles. The optimisation process for this system is described in [33]. The resolving power $m/\Delta m$ of the instrument, calculated with no regard to the Coulomb interaction, amounts to 150 000; however, the self-bunching and coalescence effects lead to the fact that the real resolving power of the instrument does not exceed 100 000.

To demonstrate the development of the self-bunching phenomenon in the oscillation process, the time-energy diagrams are presented in Fig. 4, which describe the evolution in the central plane of this multireflection system of an ion bunch consisting of 1000 ions with $m/z = 190$. The initial coordinates X_0, Y_0 of the ion trajectories are uniformly distributed in the range of $-0.6 \ldots 0.6$ mm, the initial spread of the coordinate Z_0 is set equal to zero. The initial energy and the energy spread of ions on the principal trajectory at the entrance to the injection system where the bunch acquires an energy of 500 eV, is also assumed to be zero.

Unlike the diagrams in Fig. 4 (left), where the Coulomb interaction is not taken into account, the right-hand diagrams indicate that the temporal spread of ion distributions is gradually stabilising in the process of oscillations, which is a manifestation of the self-bunching effect.
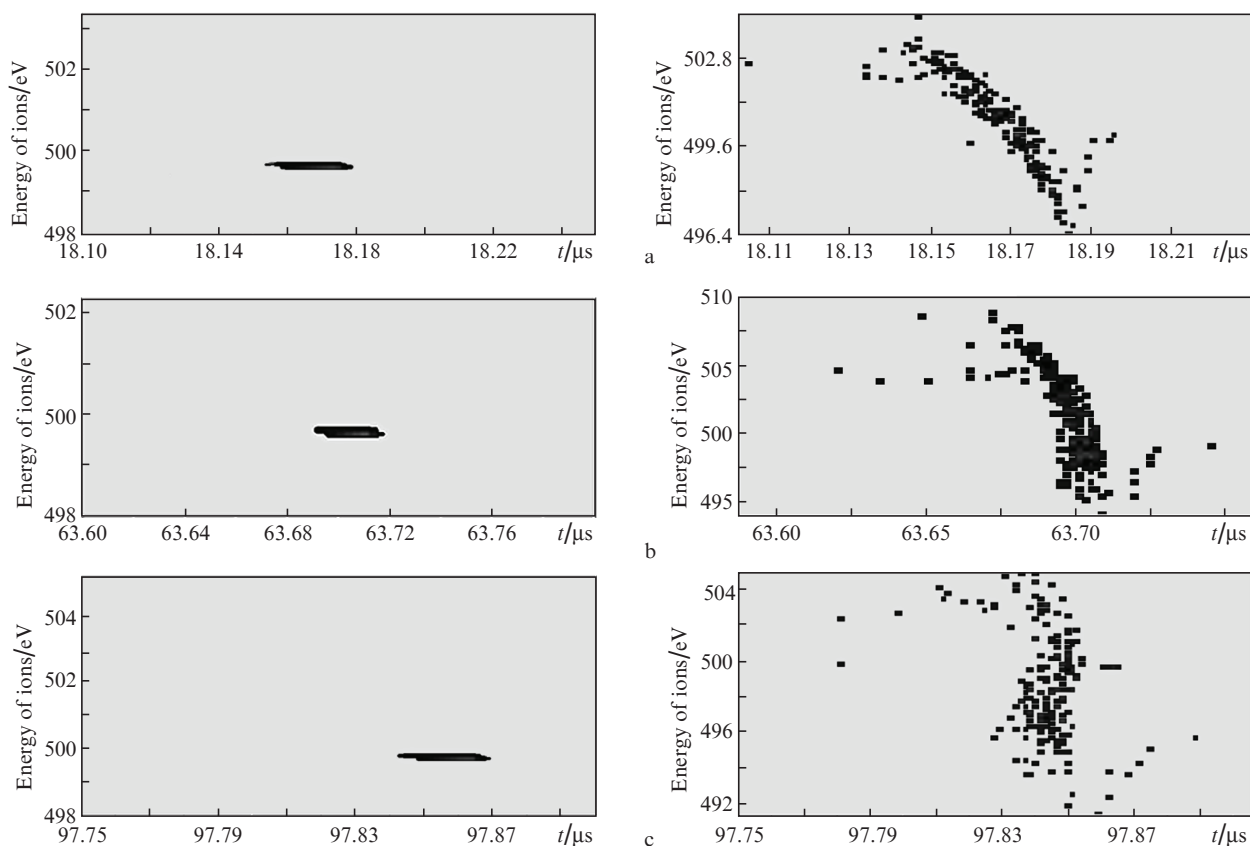

Figure 3. Structure of electrodes, axial potential distribution (dashed line) and ion trajectories (solid line) in the TOF reflectron-type mass analyser.

Figure 4. Time–energy diagrams characterising the ion bunch state in the central plane of the reflectron after (a) one, (b) three and (c) five oscillations. In the diagrams on the left, in contrast to those on the right, the Coulomb interaction is ignored.

In order to reveal the phenomenon of coalescence, which consists in resonance synchronisation of the ion motion with close m/z ratios, the ion bunch has to perform a sufficient number of oscillations. Figure 5 shows the TOF distributions in the reflectron central plane for the ion bunch comprising two groups of particles with equal number of particles and the ratio m/z = 196.00 and 196.02 (100 particles in Fig. 5a and 150 particles in Fig. 5b). Herewith, each horizontal row in Fig. 5 corresponds to one, five or nine oscillations, respectively.
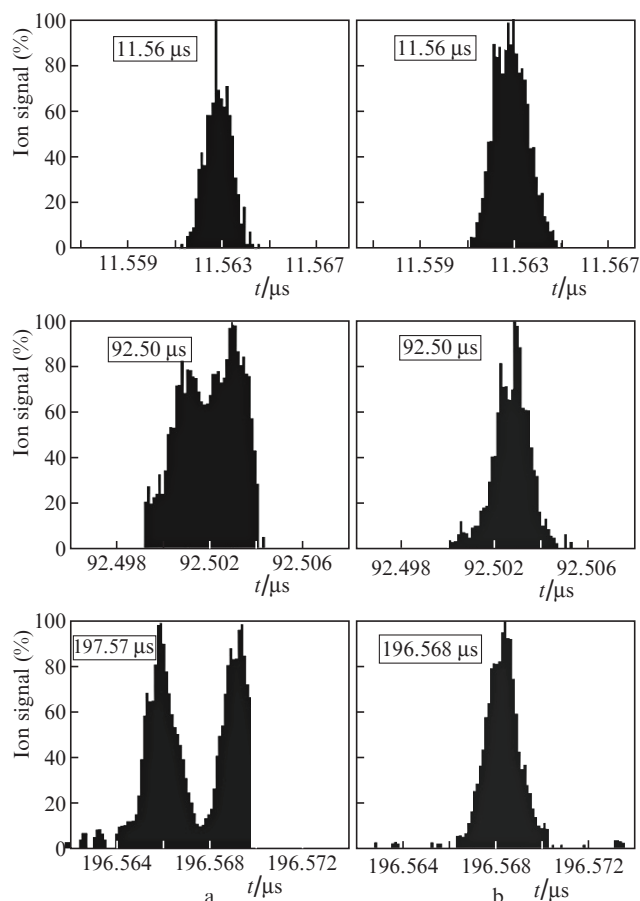

Figure 5. Evolution of the ion bunch with close m/z ratios (196 and 196.02), presented in the form of transit time diagram with account for Coulomb interaction, in the case of (a) 100 and (b) 150 elementary charges.

Evolution of the ion bunch with no regard to the Coulomb interaction between the particles represents a monotonous increase in the time interval between the particles having different m/z ratios. The calculations show that in this case the TOF difference ('divergence') between the two groups of particles after nine oscillations amounts to 8 ns.

Figure 5 shows the evolution of the same ion bunch, with the total number of charged particles equal to 100, when the Coulomb interaction is taken into account. The dynamics of the subgroups of ions is here somewhat different from the case when the Coulomb interaction is totally ignored; however, temporal 'divergence' of the particles with close m/z ratios is still observed. Since the scale graduation mark in this Figure is 2 ns, we may ascertain that the 'divergence' of the ion groups after nine oscillations constitutes 4 ns (FWHM).

In Fig. 5b the total number of interacting charged particles is already 150. It can be seen that after the total number of particles increased merely by half, the ion motion has radically changed. Both subgroups of ions are moving as a single entity, whilst the ion cloud size remains virtually unchanged. That means that the ion masses under consideration have become unresolvable. Thus, we see that the coalescence effect may significantly reduce the resolving power of the reflectron.

It is important to note that our numerical experiments point to the possibility of employing the aberrational methods in evaluation of the resolving power limitations conditioned by such phenomena as self-bunching and coalescence. A relatively small number of elementary charges (only 150) required to reveal these effects indicates that, with the use of modern ionisation methods, when the ion bunches comprising tens or even hundreds of thousands of charged particles are being analysed, the Coulomb interaction becomes a decisive factor in determining the resolving power of mass spectrometric instruments.

6. Conclusions

Theoretical approaches to the modelling of the Coulomb effects in short ion bunches, developed previously on the basis of the modified Barnes–Hut algorithm and aberration theory, have been adapted to the simulation of multireflection mass-spectrometer systems. A computational procedure for calculating the mirror potential induced by the ion bunch on the field-forming electrodes is elaborated. The algorithm determines dynamically the ion cloud location relative to the field-forming electrodes, so that only the electrode parts that directly affect the temporal and spatial characteristics of the ion bunch in the course of its motion are being involved into the calculation process.

A totality of the developed specialised computational methods and algorithms has been implemented as a separate program module of the MASIM 3D applied software package and passed through an extensive testing on the model problems. To illustrate the software efficiency, a simulation of the Coulomb dynamics of ion bunches in a TOF reflectron-type mass analyser has been performed. Numerical experiments have allowed us to reveal and study in detail the resolving power limitations due to the resonant Coulomb effects of self-bunching and coalescence as applied to the groups of charged particles with close masses.

Thus, reliable and versatile software has been created, which allows numerical optimisation of the ion optics elements with regard to the Coulomb interaction and may serve as a tool for advancing the resolving power of the modern mass-spectrometer instruments.

References

1. Mamyrin B.A., Karataev V.I., Shmikk D.V., Zagulin V.A. *Zh. Eksp. Teor. Fiz.*, **64**, 82 (1973).

2. Wollnik H., Casares A. *Int. J. Mass. Spectrom.*, **227**, 217 (2003).
3. Wollnik H., Casares A., Radford D., Yavor M. *Nucl. Instrum. Methods (A)*, **519**, 373 (2004).
4. Yavor M.I., Verenchikov A.N. *Nauchn. Priborostr.*, **14**, 38 (2004).
5. Yavor M., Verentchikov A., et. al. *Phys. Proc.*, **1**, 391 (2008).
6. Makarov A., Greenfield D. UK Patent Application, GB 2455977, 209.
7. Knight R.D. *Appl. Phys. Lett.*, **38**, 221 (1981).
8. Siegbahn K., Kholine N., Golikov G. *Nucl. Instrum. Methods (A)*, **384**, 563 (1997).
9. Makarov A. *Anal. Chem.*, **72**, 1156 (2000).
10. Makarov A., Giannakopulos A. US Patent US2012138785.
11. Alexandrov M.L., Gall L.N., Krasnov N.V., Nikolaev V.I., Shkurov V.A. *Dokl. Akad. Nauk SSSR*, **277**, 379 (1984).
12. Yamashita M., Fenn J.B. *J. Phys. Chem.*, **88**, 4451 (1984).
13. Karas M., Bachmann D., Bahr D., Hillenkamp F. *Int. J. Mass Spectrom. Ion Proc.*, **78**, 53 (1987).
14. Tanaka K., Waki H., Ido Y., Akita S., Yoshida Y., Yoshida T., Matsuo T. *Rapid Commun. Mass Spectrom.*, **2**, 151 (1988).
15. Tal'roze V.L., Lyubimova A.L. *Dokl. Akad. Nauk SSSR*, **86**, 909 (1952).
16. Revelskii I., Yashin Y., Kurochkin V., Kostyanovskii R. *Industrial Laboratory*, **57**, 243 (1991).
17. Cody R.B., Laramée J.A., Durst H.D. *Anal. Chem.*, **77**, 2297 (2005).
18. Jabin S.N., Pento A.V., Grechnikov A.A., Borodkov A.S., Sartakov B.G., Simanovskiy Ya.O, Alimpiev S.S. *Kvantovaya Elektron.*, **41**, 835 (2011) [*Quantum Electronics*, **41**, 835 (2011)].
19. Pento A.V., Nikiforov S.M., Simanovskiy Ya.O., Grechnikov A.A., Alimpiev S.S. *Kvantovaya Elektron.*, **43**, 55 (2013) [*Quantum Electronics*, **43**, 55 (2013)].
20. Huygens C. *Letter to de Sluse*. In: *Oeuveres Complètes de Christian Huygens* (letters; no. 1333 of 24 February 1665, no. 1335 of 26 February 1665, no. 1345 of 6 March 1665) (La Haye: Societe Hollandaise Des Sciences, Martinus Nijhoff, 1888–1950).
21. Pedersen H.B., Strasser D., Ring S., Heber O., Rappaport M.L, Rudich Y., Sagi I., Zajfman D. *Phys. Rev. Lett.*, **87**, (5), 055001 (2001).
22. Pedersen H.B., Strasser D., Amarant B., Heber O., Rappaport M.L., Zajfman D. *Phys. Rev. A*, **65**, 042704 (2002).
23. Zajfman D., Rudich Y., Sagi I., Strasser D., Savin D.W., Goldberg A.S., Rappaport M.L., Heber O. *Intern. J. Mass Spectrom.*, **229**, 55 (2003).
24. Bolotskikh P.A., Grinfeld D.E., Makarov A.A., Monastyrskiy M.A. *Nucl. Instrum. Methods (A)*, **645**, 146 (2011).
25. Kharchenko A., Vladimirov G., Heeren R., Nikolaev E. *J. Am. Soc. Mass Spectrom.*, **23** (5), 977 (2012).
26. Kozlov B.N., Kirillov S.N., Monakhov A.M. *Mass Spektrom.*, **9**, 223 (2012).
27. Vladimirov G., Hendrickson C.L., Blakney G.T., Marshall A.G., Heeren R.M., Nikolaev E.N. *J. Am. Soc. Mass Spectrom.*, **23**, 375 (2012).
28. Greenfield D.E., Monastyrskiy M.A., Tarasov V.A. *Software Demonstrations Abstract Book, 'CPO-7' Intern. Conf.* (Cambridge, UK: Cambridge, 2006) p. 23.
29. Barnes J., Hut P. *Nature*, **324**, 446 (1986).
30. Grinfeld D.E., Monastyrskiy M.A. *Phys. Procedia*, **1**, 217 (2008).
31. Greenfield D., Monastyrskiy M. *Selected Problems of Computational Charged Particle Optics* (Netherlands: Elsevier, AIEP, 2009).
32. Bykov V.P., Gerasimov A.V., Turin V.O. *Usp. Fiz. Nauk*, **165**, 955 (1995).
33. Grinfeld D., Giannakopulos A., Kopaev I., Makarov A., Monastyrskiy M., Skoblin M. *Europ. J. Mass Spectrom.*, **20**, 131 (2014).